Dalton Transactions

Accepted Manuscript

ROYAL SOCIETY OF CHEMISTRY

www.rsc.org/dalton

Dalton Transactions

ARTICLE

Electrochemical Fabrication of Copper-Containing Metal–Organic Framework Films as Amperometric Detectors for Bromate Determination

Received 00th January 20xx,
Accepted 00th January 20xx

DOI: 10.1039/x0xx00000x

www.rsc.org/

Erbin Shi[a], Xiaoqin Zou[b], Jia Liu[c], Huiming Lin[a], Feng Zhang*[a], Shaoxuan Shi[a], Fenghua Liu[a], Guangshan Zhu[b] and Fengyu Qu*[a]

A facile electrochemical plating strategy has been employed to prepare the electroactive metal-organic framework film (NENU-3) onto a copper electrode in the acid electrolyte containing 1, 3, 5-benzenetricarboxylic acid (H_3BTC) and phosphotungstic acid (PTA). The as-made NENU-3 films have been characterized using powder X-ray diffraction (PXRD), scanning electron microscopy (SEM), Fourier transform infrared (FT-IR) and thermogravimetric analyses (TGA). These analyses indicate that NENU-3 films have high phase purity and high stability. Further, different electrochemical techniques are utilized for measuring the electrochemical behaviors of the NENU-3 film electrodes. Accordingly, the kinetic parameters for NENU-3 film electrode towards electrocatalytic reduction of bromate are obtained, including the electron transfer coefficient (α), the catalytic rate constant (k_s), and the diffusion coefficient (D). The film electrodes present excellent electrocatalytic ability for the bromate reduction, and can be used successfully for amperometric detection of bromate. Under the optimized conditions, the proposed sensor exhibits a wide linear range (0.05 ~ 72.74 mM) and a lower detection limit (12 μM) measured by chronoamperometry (CA). Moreover, the films possess high electrochemical stability and strong anti-interference capability in bromate detection process. It has been demonstrated that the electrochemical plating method reported here offers a reliable and effcient way to fabricate MOF films on conductive substrates for bromate detection.

Introduction

Metal-organic frameworks (MOFs) are emerging as a new family of molecular sieve materials, which are constructed by metal ions or clusters and a variety of organic linkers into highly porous frameworks.[1-3] The various organic ligands and inorganic components enable molecular engineering of MOFs with topologically diverse and pleasing structures.[4] Besides the versatile applications in gas storage and separation,[5-6] catalysis,[7] optics,[8] MOFs are attractive for being assembled into films which principally display practical functionalities superior to their bulk crystalline materials.[9-11] In particular, the molecular detections based on MOF films are seen with absorbing applications for magnetic films,[12-13] proton/electron-conducting films,[14-17] optical devices,[18-20] and redox-active sensors.[20-23] However, compared to the other sensing applications mentioned above, only a few studies have been conducted them to investigate electrochemical detection.[23-25]

Very recently, a small number of studies have been trying to apply MOF bulk crystals as the electroactive materials for detecting trace amounts of the compounds due to the unique properties of MOFs including various pore size, high surface area, specific adsorption affinity and naked active site,[26-30] which make MOFs good biosensor candidates for electrochemical reactions. Therefore, the exploration of MOF-based films as novel electrochemical detectors is attracting growing interests although it is still in a relatively new research field and remains a significant challenge.

In recent years, many efforts have been directed towards choosing the proper synthetic strategies for the formation of MOF films,[31] which are also important for utilizing MOF materials in thin-film sensors and electrochemical devices. In general, MOF films can be prepared by several methods, such as solvothermal method and slow solution diffusion.[32-33] In these synthetic methods, multiple steps, long synthesis time and the pretreatment of substrate surfaces are required. As a result, the development of a universal method for MOF film formed is a main target in this research area. More recently, a few successful examples have been reported by employing electrochemical route to fabricate MOF films.[34-41] Compared with conventional routes, this method offers a facile, environmentally friendly, and easy scale up way for the preparation of the MOF films.[34] Also, the electrosynthetic process affords the film deposition progress to be monitored

[a] College of Chemistry and Chemical Engineering, Harbin Normal University, Harbin, Heilongjiang 150025 (P. R. China) E-mail:qufengyuhsd@163.com; zhangfeng_chem@aliyun.com; Tel. /fax: +86 451 88060653
[b] Key Laboratory of Polyoxometalate Science of the Ministry of Education, Faculty of Chemistry, Northeast Normal University, Changchun, Jilin 130024 (P.R. China)
[c] College of Chemistry, Jilin University, Changchun, Jilin 130012 (P.R. China)
Electronic Supplementary Information (ESI) available.
See DOI: 10.1039/x0xx00000x

by a change in an applied voltage or current, giving control over film thickness.[37] Moreover, it is an effective technique to address the challenge of interfacing MOF layers with the surfaces of the conductive substrates in the electrochemical application.[36]

Detection of bromate, a group B-2 carcinogen classified by the International Agency for Research on Cancer (IARC), is of great interest owing to its health and environmental implications.[42] Among numerous analytical techniques for the determination of bromate,[42-43] electrochemical approach is considered attractive because of its environmentally friendly procedure, short response time, often efficient cost and feasibility for building portable sensors.[44-45] In this regard, intensive research efforts have been devoted to explore direct electrochemistry-based materials to be applied in detecting bromate electrochemically.

Herein, our interest is to employ electrochemical technique for the preparation of MOF films and to investigate their electrochemical performances for the electroreduction of bromate. The feasibility of this concept has been exemplified by choosing an electroactive MOF (NENU-3) as the target material,[46-47] composed of $Cu_3(BTC)_2$ encapsulating Keggin-type heteropolyacid, phosphotungstic acid (PTA). The framework of $Cu_3(BTC)_2$ has an intersecting three-dimensional network containing two kinds of pores (9 ~ 13 Å), and holds good mechanical property and high adsorption affinity (**Figure S1**).[48] Meanwhile, the PTA occluded in half of the $Cu_3(BTC)_2$ pores makes NENU-3 structure more robust in aqueous solution compared to $Cu_3(BTC)_2$,[49] which is very important in view of electrochemical detection. Moreover, PTA as a strong electrolyte can enhance charge transport in the reaction media for electrochemical plating, and thus avoid the introduction of other electrolytes. Additionally, the obtained NENU-3 films are comprehensively characterized by powder X-ray diffraction (PXRD), scanning electron microscopy (SEM), Fourier transform infrared spectroscopy (FT-IR) and thermogravimetric (TGA). The electrochemistry and electron transfer kinetics of NENU-3 films towards the reduction of bromate are also investigated by different electrochemical techniques, and finally the analytical performances of the films are described as an amperometric sensor for the detection of bromate.

Experimental section

Chemicals and Reagents

1, 3, 5-benzenetricarboxylic acid (H_3BTC, 99%), sodium bromate ($NaBrO_3$, 99%) were purchased from Sigma Aldrich and used as supplied. Copper plates (99.9% copper), and phosphotungstic acid (PTA, 99%) were obtained from Aladdin Company. The Britton-Robinson (B-R) buffer solution made up from boric acid (H_3BO_3), acetic acid (HAc), phosphate (H_3PO_4) and sodium hydroxide (NaOH) was employed as a supporting electrolyte. Other reagents and chemicals were used without further purification, and all chemical solutions and experiment procedures were prepared with double distilled, deionized (DDDI) water and stored at room temperature.

Electrochemical Synthesis of NENU-3 Film

Prior to the preparation of NENU-3 films, the copper plates used as the substrates were cut into rectangle wafers (2.5 × 3.0 cm^2), rinsed with acetone and then washed with ethanol for three times under ultrasonic vibration for 10 min, respectively, and then stored in pure ethanol solution. Before use, they were taken out and dried in air.

For the electrodeposition experiment, as-pretreated copper plate and platinum slice used as anode and cathode respectively were mounted in a custom-made polypropylene holder. The synthetic mixtures containing H_3BTC (0.583 g, 2.78 mmol), PTA (0.800 g, 0.278 mmol) were dissolved in ethanol (20 mL) and water (20 mL). A copper plate (2.5 × 2.5 cm^2) was submerged and exposed to the deposition bath. By applying a voltage (2 V) using a direct current (DC) power source for 2 h, NENU-3 film was then grown on the anode at room temperature. After the film growth, the coated copper plate was removed from the holder and gently rinsed using ethanol and water several times to remove excess ligand and PTA before drying at room temperature overnight.

Instruments

The crystalline structures of the films and powders were determined by powder X-ray diffraction (PXRD) measurements using Riguku D/MAX2550 diffractometer with Cu K_α radiation (λ = 1.5418 Å) at 50 kV and 200 mA. The morphologies of the as-prepared films were observed by field-emission scanning electron microscopy (SEM) performed using JEOS JSM6700F. The Fourier transform infrared spectra (FT-IR) were collected on a Bruker IF66F/V FTIR spectrometer at room temperature in the range of 400 ~ 4000 cm^{-1}, with potassium bromide pellets. Thermogravimetric analyses (TGA) of the samples were performed on a Perkin-Elmer TGA 7 thermogravimetric analyzer from room temperature to 600 °C with a heating rate of 5 °C/min in air. Nitrogen adsorption-desorption measurement on the NENU-3 powders was carried out at 77 K by using an Autosorb iQ2 adsorptometer, Quantachrome Instruments. Prior to the tests, as-synthesized NENU-3 was degassed under vacuum overnight at 150 °C. Specific surface area was determined using the Brunauer-Emmett-Teller (BET) equation over the range of relative pressures P/P_0 between 0.05 and 0.3. The pH values were measured on a model PHSJ-4F digital acidometer with precision of 0.001.

Electrochemical Measurements

A CHI 660D electrochemical analyzer (CH Instruments, Shanghai Chenhua Instrument Corporation, China) and a PARSTAT 4000 electrochemical workstation (Princeton Applied Research, Princeton, NJ, USA) were employed for electrochemical measurements in a conventional three-electrode cell with a NENU-3 film supported on the copper substrate as the working electrode, a saturated calomel electrode (SCE, saturated KCl aqueous) as the reference electrode, and a platinum wire as the counter electrode in B-R buffer solution electrolyte (pH 6.5). All the potentials were measured and reported versus SCE. In this study, all the

sample solutions were purged with purified argon (Ar) for at least 20 min to remove oxygen (O_2) prior to the experiments and all the tests were carried out at ambient temperature with purging Ar throughout every experiment process.

Results and discussion

3.1 NENU-3 Films and General Characterizations

The PXRD pattern collected from the NENU-3 film *via* electrochemical synthesis is shown in **Figure 1**. As depicted in **Figure 1**, the diffraction pattern of the NENU-3 film (**Figure 1b**) is well matched with the simulated one (**Figure 1a**) by judging all appeared peaks positions,[46] indicating that highly crystalline NENU-3 crystals are grown on the copper substrate. No characteristic reflections of the copper plate are observed, suggesting a good coverage of the substrate by the NENU-3 layer.

The optical picture of NENU-3 film prepared on a copper substrate is shown in **Figure 2d**. The sapphire colour indicates that the substrate is entirely covered by the NENU-3 crystal layer. The surface morphology of the as-prepared NENU-3 films is monitored by SEM (**Figure 2a-c**). After 2 hours' electrochemical plating treatment, octahedral NENU-3 crystals with a size of 3 ~ 4 μm are well integrated on the surface of the copper plate (**Figure 2a**). With a close look, the high-quality NENU-3 film without visible cracks is obtained, which is confirmed by a magnified top view in **Figure 2b**. The cross-sectional SEM image of the film shows that the crystals anchor to the copper substrate tightly (**Figure 2c**), which is in good agreement with the surface images (**Figure 2a and b**). Meanwhile, the thickness of the NENU-3 film is estimated to be about 4 μm, a roughness comparable with the size of the individual crystals.

Thermal gravimetric analysis (TGA) is a fundamental and effective method to examine the thermal stability of porous materials. The TGA and corresponding differential thermal gravity (DTG) curves of the $Cu_3(BTC)_2$ and NENU-3 are presented in **Figure S2**. As expected, NENU-3 exhibits a lower weight loss than $Cu_3(BTC)_2$ as Keggin-type PTA is incorporated in $Cu_3(BTC)_2$ during electrochemical synthesis. Compared with the reference curve of the $Cu_3(BTC)_2$, there is a slightly delayed weight loss for the NENU-3 between 300 ºC and 335 ºC, which is possibly attributed to the presence of Keggin ions between parallel layers of $Cu_3(BTC)_2$, and consequently enhance the thermal stability of the NENU-3 material.[50] The results show

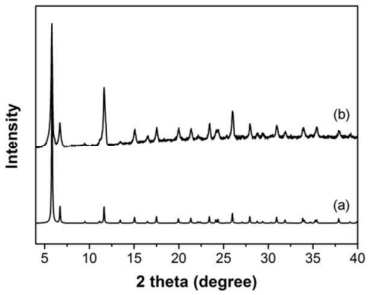

Figure 1. PXRD patterns of (a) the simulated NENU-3 material and (b) the as-made NENU-3 film.

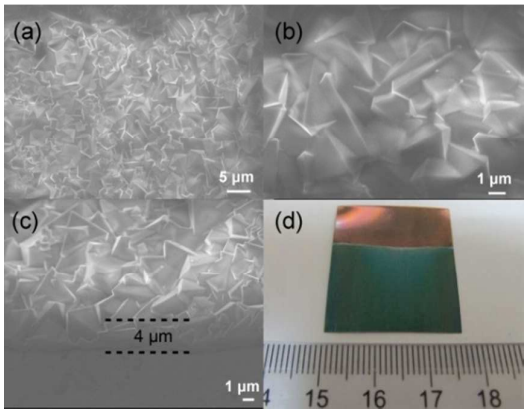

Figure 2. SEM images of (a) the NENU-3 film, (b) an enlarged view of the NENU-3 film, and (c) the cross-sectional view of the film. (d) Optical picture of the NENU-3 film grown on the copper substrate.

the slightly higher thermal stability of NENU-3 than that of pure $Cu_3(BTC)_2$, which could bring a benefit for practical application of electrochemical detection.

In order to demonstrate the aqueous stability of NENU-3, the as-synthesized NENU-3 film was placed in a vial containing the water. The mixture was agitated at room temperature on a shaker and then analyzed using PXRD (**Figure S3 and S4**). Upon immersion in water, the PXRD pattern of $Cu_3(BTC)_2$ completely changes over a period of 15 min (**Figure S3**), indicating that major structural changes are taking place. In contrast, minimal changes are occurred in the PXRD pattern of NENU-3 film after immersion in water for 24 h (**Figure S4**), which suggests that the crystalline structure for the NENU-3 material is stable in water for that time period. It is because that due to the presence of PTA between parallel layers of the NENU-3, any disintegration of structure is prevented, and consequently locks the skeleton structure.[50] In addition, the water solution in which the NENU-3 was examined for dissolved material was also checked by ^{1}H NMR and ICP analysis. Only water peak was observed in the ^{1}H NMR spectrum of the aqueous (**Figure S5**). The only small amounts of Cu^{2+} (0.109 mM) in the water solution were detected by ICP analysis, and a mass loss of 2.4% is calculated according to the formula of NENU-3 ($[Cu_{12}(BTC)_8][H_3PW_{12}O_{40}]$). The water stability of NENU-3 may extend its useful applications in electrochemical sensing.

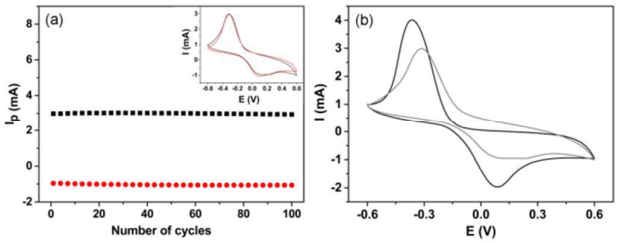

Figure 3. (a) Run number dependence of the redox peak current (I_p) for the NENU-3 film electrode in pH 6.5 B-R buffer solution at a scan rate of 50 mV s^{-1}; inset: the voltammograms of the NENU-3 film electrode for the different run numbers (1st and 100th). (b) Cyclic voltammograms of the NENU-3 film electrode in the absence (gray) and the presence (black) of 0.3 mM bromate under the condition as (a).

3.2 Electrochemical characterization of the NENU-3 film electrodes

Inspired by the successful preparation of the NENU-3 films and their stabilities, we further employed to evaluate the electrochemical properties of the films. At first, the basic voltammetric responds of the bare copper substrate and the NENU-3 film electrode for the reduction of bromate were investigated by using cyclic voltammetry (CV) in the potential range of -0.6 to +0.6 V. (**Figure 3b and S6**). Upon the addition of 0.3 mM of bromate, the change of the current signal for the reduction of bromate is negligible for the bare copper substrate. While, for the NENU-3 film electrode, there are marked increases of the anodic and cathodic currents, respectively, suggesting that the NENU-3 crystals on the film exhibits excellent electrocatalytic behaviours for the reduction of bromate in the B-R buffer solution (pH 6.5). Meanwhile, the NENU-3 film displays an oxidation peak at +0.15 V and a reduction peak appeared approximately at -0.315 V in the CV response (**Figure 3b**). This redox signal may be attributed to the redox process of Cu^{II}/Cu^{I} in the NENU-3 structure.[51] The NENU-3 material is conductive (4.76×10^{-5} S cm^{-1} at 90 °C under 70% relative humidity)[52], and the unsaturated coordinated metal center in the MOF structure could be used as the active center of the electrocatalyst,[46] which could result in the redox activity and the change of the signal current of NENU-3 film electrode for the reduction of bromate. Additionally, the electrochemical stability of NENU-3 film electrode is also checked by using CVs. To be noted, the NENU-3 film electrode displays only a slight change of voltammetric peak current after 100 cycles (**Figure 3a**). It is found that the peak current still remains about 97% of the initial value after 100 cycles, which suggests that the NENU-3 film electrode has a good cycling stability for practical sensing application.

The effect of solution pH on the electrochemical response of the NENU-3 film electrode to 0.3 mM bromate was investigated in the buffer solution at the pH range from 5.0 to 7.5 by the linear sweep voltammograms (LSVs) (**Figure 4**). As shown in **Figure 4a**, the NENU-3 film electrode can catalyse the electro-reduction of bromate at pH value from 5.0 to 7.5. It can be well observed that the cathodic peak current of the film in the presence of bromate increases gradually with an increase of pH value until it reaches the maximum at pH 7.0 (**Figure 4a inset**). Considering the sensitivity of the detection of bromate on the surface of NENU-3 film electrode, a pH of 6.5 is chosen for the subsequent analytical experiments. The relationship between the peak potential (E_p) and pH value is illustrated in **Figure 4b**. The E_p value gradually shifts to more negative with the pH increase of the supporting electrolyte solution, which is possibly attributed to the participation of protons in the electrode reaction. In the pH range from 5.0 to 7.5, E_p follows the linear regression equations with pH: E_p (V) = -0.079pH + 0.153 (r = 0.995). According to the following formula[53]:

$$dEp/dpH = -2.303\ mRT/nF \qquad (1)$$

where n and m are the electron transfer number and the number of protons participating in the electrochemical reaction, respectively. The ratio of m/n for NENU-3 film is approximately to 1, indicating that the electron transfer is accompanied by an equal number of protons in the electrochemical reaction of bromate.

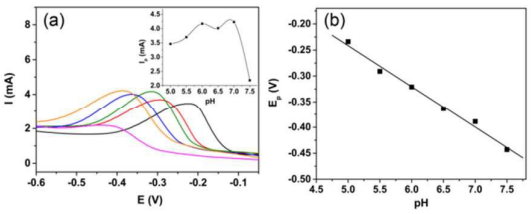

Figure 4. (a) LSVs of the NENU-3 film electrode in the presence of 0.30 mM bromate under the different pH values, and (a, inset) the effect of pH on the peak current and (b) the peak potential in the B-R buffer solution at a scan rate of 50.0 mV s^{-1}.

Generally, the useful data involving the electrochemical mechanism can be obtained from the potential scan rate studies. Thus, the influence of redox peak for the NENU-3 film electrode on the electrochemical reduction of bromate was recorded by CV on different scan rates at a potential range of -0.6 ~ 0.6 V in the B-R buffer solution (pH 6.5) (**Figure 5**). It can be observed that varying the scan rates from 10 to 100 mV s^{-1} results in a gradual increase of redox peak current of the film electrode (**Figure 5a**). The redox peak separation is greatly enhanced as a function of the scan rate for the film electrode. The linear regression equations about the redox peak currents upon the square root of scan rate ($\upsilon^{1/2}$) are expressed as follows: I_{pc} (mA) = 0.4293 + 0.4977$\upsilon^{1/2}$ (mV $s^{-1})^{1/2}$ (r = 0.9994) and I_{pa} (mA) = 0.00678 - 0.2794$\upsilon^{1/2}$ (mV $s^{-1})^{1/2}$ (r = 0.9997), indicating that a diffusion-controlled behavior for the electro-reduction of bromate on the surface of the NENU-3 film electrode (**Figure 5b**). In addition, the peak potential ($|E_p|$) increases linearly with an increase of the natural logarithm of scan rate (lnυ) (**Figure 5c**), which suggests that the electro-reduction of bromate for the NENU-3 film electrode is irreversible. For the irreversible electron-transfer electrode process, the information on the rate determining step can be obtained from the following Laviron's equation[53-54]:

$$E_{pc} = E^{0'} + \frac{RT}{\alpha n_\alpha F} ln\left(\frac{RTk_s}{\alpha n_\alpha F}\right) - \frac{RT}{\alpha n_\alpha F} ln\nu \qquad (2)$$

$$E_{pa} = E^{0'} - \frac{RT}{(1-\alpha) n_\alpha F} ln\left(\frac{RTk_s}{(1-\alpha) n_\alpha F}\right) + \frac{RT}{(1-\alpha) n_\alpha F} ln\nu \qquad (3)$$

$$ln\, k_s = \alpha ln(1-\alpha) + (1-\alpha) ln\,\alpha - ln\left(\frac{RT}{n_\alpha F \upsilon}\right) - \frac{(1-\alpha)\alpha n_\alpha F \Delta E_p}{RT} \qquad (4)$$

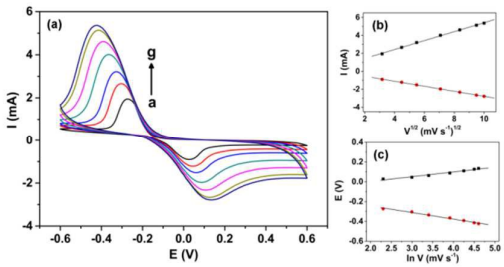

Figure 5. (a) CV responses of the NENU-3 film electrode in the B-R buffer solution (pH 6.5) at the different scan rates in the absence of 0.3 mM bromate: (from a to g) 10, 20, 30, 50, 70, 90, and 100 mV s^{-1}. The plots of (b) the peak current vs. the square root of scan rate ($\upsilon^{1/2}$) and (c) the peak potential vs. the lnυ.

where $E^{0'}$ is the formal potential, α is referred to the electron-transfer coefficient, n_α stands for the electron number involved in the rate-determining step, υ is the scan rate, k_s is the standard heterogeneous rate constant of the surface reaction, and R, T, and F have their usual meaning. As displayed in **Figure 5c**, the plots of E_p versus lnυ are linear:

E_{pa} (V) = - 0.0922 + 0.0478lnυ (mV s^{-1}) (r = 0.985)

E_{pc} (V) = - 0.112 + 0.0663lnυ (mV s^{-1}) (r = 0.994)

According to the slope value of E_{pa} and E_{pc} versus lnυ, $(1-\alpha)n_\alpha$ and αn_α are calculated to be 0.54 and 0.39, respectively; and according to **Eq. 4**, k_s is 1.22 × 10^{-3} s^{-1}. In addition, αn_α value for the irreversible electrode process is also obtained using another method from the below equation:

$$E_p - E_{p/2} = \frac{1.857RT}{\alpha n_\alpha F} = \frac{0.0477}{\alpha n_\alpha} \qquad (5)$$

where $E_{p/2}$ is the potential corresponding to $I_{p/2}$. The average value for αn_α is estimated to be 0.57 at a scan rate of 10 ~ 100 mV s^{-1} for 0.3 mM bromate (**Figure 5a**), indicating that the rate-limiting step is one electron transfer with α of 0.57. The comparison of the obtained α values from two equations (**Eq. 2 and 5**) shows that the obtained results are a good agreement. Considering that the number of electron and proton involved in the electro-reduction is equal (**Figure 4**), the electrochemical reduction of bromate at the NENU-3 film electrode is identified as one-electron and one-proton step in pH-dependent electrochemical response. Besides, from the plot of peak current (i_P) versus $\upsilon^{1/2}$, the number of electrons (n) in the overall reaction can be obtained according to the following valid equation for irreversible diffusion-controlled process[53]:

$$i_p = (0.4958\times 10^{-3})nF^{3/2}(RT)^{-1/2}(\alpha n_\alpha)^{1/2}AcD^{1/2}\upsilon^{1/2} \qquad (6)$$

where A stands for the effective microscopic areas of the working electrode, c presents the bromate concentration and D is the diffusion coefficient. The slope calculated from the plot of i_{pc} versus $\upsilon^{1/2}$ (**Figure 5b**) is found to be 1.57 × 10^{-2} (A cm^{-2})/(V s^{-1})$^{1/2}$, and the effective areas (A) and the diffusion coefficient (D) are estimated to be approximately 4.62 cm^2 and 6.20 × 10^{-5} cm^2 s^{-1}, respectively (calculated below by the Anson equation), and then the total number of electrons n = 6.4 involved in the reduction of bromate could be calculated, which is identical to the result obtained by the Anson equation.[55] Accordingly, the overall reduction reaction of bromate can be written as $BrO_3^- + H^+ + 6e^- \rightarrow Br^- + H_2O$.

The electrochemically effective microscopic area of the NENU-3 film electrode could be estimated by the slope of the plot (Q versus $t^{1/2}$) using the chronocoulometric response of $K_3[Fe(CN)_6]$ solution (0.1 mM) as model complex based on the below equation given by Anson[56]:

$$Q(t) = 2nFAcD^{1/2}\pi^{-1/2}t^{1/2} + Q_{dl} + Q_{ads} \qquad (7)$$

where A is the effective microscopic areas of the working electrode, n is the number of electron transfer, D is the diffusion coefficient, c is the concentration of substrate, Q_{dl} is the double layer charge which could be eliminated by background subtraction, Q_{ads} is the Faradaic charge and could be obtained by the intercept of the Anson's plot after the subtraction of background, and other symbols have their usual meanings. The chronocoulometric curve of the film electrode in $K_3[Fe(CN)_6]$ solution (0.1 mM, 0.1 M KCl) is displayed in

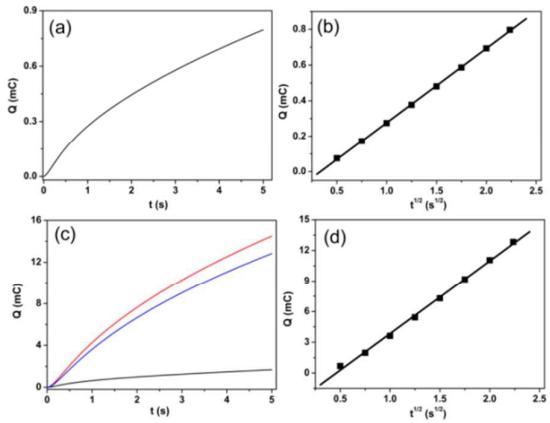

Figure 6. (a) Chronocoulometry response of the NENU-3 film electrode in the $K_3[Fe(CN)_6]$ solution (0.1 mM, 0.1 M KCl) and (b) the Q-$t^{1/2}$ curve on the NENU-3 film electrode under the condition as (a). (c) Chronocoulometry response of the NENU-3 film electrode in the absence (black) and the presence (red) of 0.3 mM bromate at the B-R buffer solution (pH 6.5) and the Q-t curve of NENU-3 film electrode after the background subtracted (blue). (d) The Q-$t^{1/2}$ plot on the NENU-3 film electrode after the background subtracted.

Figure 6a. According to Anson's equation (**Eq. 7 and Figure 6b**), the effective microscopic area of the NENU-3 film electrode can be calculated to be 4.62 cm^2 when assuming the D value of $K_3[Fe(CN)_6]$ approximately equal to that of in the bulk solution (7.6 × 10^{-6} cm^2 s^{-1}, 0.1 M KCl).[53] It is found the effective surface area for the film electrode is increased obviously after the electrode modification compared to the geometric area of working electrode (0.5 cm^2), possibly originating from the pores of the NENU-3 structure (S_{BET} = 373.09 m^2 g^{-1}) (**Figure S7**). The enlarged electrode surface can increase the electrode reaction sites, enhance the adsorption capacity, and amplify the current response of bromate and thus improve the determination sensitivity.[57] The diffusion coefficient (D) and the adsorption capacity (Γ_s) of bromate at the NENU-3 film electrode are also determined by the slope and intercept of the plot of Anson curves (**Figure 6c and d**). After the background subtraction, the plot of Q vs. $t^{1/2}$ for the NENU-3 film electrode displays a linear relationship using the slope of 7.13 mC $s^{-1/2}$ and intercept (Q_{ads}) of 3.28 mC (**Figure 6d**). Based on the above results , D value is 6.20 × 10^{-5} cm^2 s^{-1} (assuming the total number of electrons of n = 6) [55]. The Γ_s of bromate at NENU-3 film electrode could be also evaluated (1.23 × 10^{-9} mol cm^{-2}) according to the equation of $Q_{ads} = nFA\Gamma_s$.

For better understanding of the role of the NENU-3 film toward the reduction of bromate, the adsorption isotherms for bromate and the competing analytes (e.g. chloride and bromide) were recorded at 298 K (**Figure S10, S11 and S13**). It is found that the NENU-3 material shows a relatively high uptake of bromate (**Figure S10**). The uptakes of chloride and bromide on the NENU-3 material are 0.0041 μmol L^{-1} (**Figure S11**) and 0.00032 μmol L^{-1} (**Figure S13**) at the initial concentrations of 0.28 mmol L^{-1} and 0.31 mmol L^{-1}, respectively, which are less than that of bromate (0.078 μmol L^{-1}) at the initial concentration of 0.31 mmol L^{-1}. The result

shows that the NENU-3 material has a relatively high affinity for bromate, compared with those of the competing analytes (chloride and bromide). Combining the above quantitative analysis, it can be deduced that the electrocatalytic reduction of bromate on the conductive NENU-3 film electrode would probably be ascribed to its larger effective surface area and the stronger adsorption affinity of bromate arising from the pores and coordinately unsaturated active sites of NENU-3.

3.3 Detection of bromate at NENU-3 film electrode

Chroamperometry (CA) as an electroanalytical method with a highly sensitive and a low detection limit is used to estimate the detection of bromate. In order to obtain an optimum potential for the reduction current on the NENU-3 film, multi-potential steps are applied between 0 and -0.4 V. The experimental results show that the amperometric current varies with the applied potential to the electrode, and the maximum current is obtained at -0.3 V. **Figure 7** shows a typical current-versus-time curve of the NENU-3 film for the successive injections of bromate added at an applied potential of -0.3 V in the range from 0.05 mM to 72.74 mM into a stirred B-R buffer solution (pH 6.5) under the ambient condition. When an aliquot of bromate is added into the stirring solution, the reduction current increases rapidly to reach 98% of the steady state current within 8 s (**Figure 7a**).[58] The relatively fast response is mainly attributed to the thin active film and the quick penetration of bromate. It is also noticeable that the noise increases at high bromate concentration, which is possibly related to more and more intermediate species adsorbed onto the NENU-3 film electrode as the bromate concentration and the reaction time increase. The relationship between the response current of the NENU-3 film electrode and the concentration of bromate is depicted in **Figure 7b**. It can be seen that an increase in the bromate concentration is accompanied by an increase in cathodic current, and two linear sections in the regression line fit the following equations: for the concentrations in the range from 0.05 to 19.10 mM, I (mA) = 0.179 + 0.0519c (mM) (r = 0.997), and for the concentrations in the range from 19.10 to 72.74 mM, I (mA) = 0.692 + 0.0235c (mM) (r = 0.998) (**Figure 7b**). The calculated limit of detection (LOD) is 12 μM (based on $3S_b/S$, where S_b is the standard deviation of 10 measurements taken from the signal obtained from the blank, S is the slope of the calibration curve, and the number 3 comes from the required 90% level of confidence in the difference between the observed signal and the blank response) for reduction bromate at the film electrode. The linear calibration range and LOD of the film electrode are close to or even better than those of other documented examples of typical modified electrodes (Table S1).[59-60] Additionally, the sensitivities of the sensor are founded equal to 11.2 μA mM^{-1} cm^{-2} (0.05 ~ 19.10 mM) and 5.08 μA mM^{-1} cm^{-2} (19.10 ~ 72.74 mM), respectively, from the slope of the calibration curve. These results indicate that the NENU-3 film electrode is acceptable for the amperometric

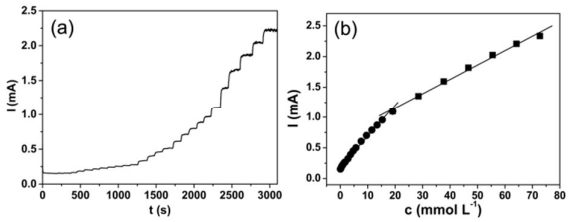

Figure 7. (a) Typical amperometric current–time response of the NENU-3 film electrode upon the sequential addition of bromate with the different concentration in the pH 6.5 B-R buffer solution at a potential -0.3 V. (b) The calibration curves of the current response vs. the bromate concentration under the condition as (a).

determination of bromate in a concentration region of 0.05 ~ 72.74 mM, demonstrating that the electroactive NENU-3 material could be used as a valid candidate for bromated detection from a practical point of view.

3.4 Anti-interference and stability of the NENU-3 film electrode

One of the important analytical factors for a sensor is its ability to discriminate the common coexisting ions with the target analytes in real samples.[61] Therefore, the influences of some possible interfering substances are studied on the performance of proposed sensor. The interferential experiment of the fabricated bromate sensor based on NENU-3 film is performed by comparing the amperometric response of 0.1 mM bromate before and after adding some possible interferents at fixed potential (-0.3 V) into the B-R buffer solution (pH 6.5). The current ratio of the amperometric response of the mixtures (1 mM) each interfering substance in the presence of 0.1 mM bromate compared to that of 0.1 mM bromate alone is taken as the criterion for the selectivity of the bromate sensor. As can be seen from **Table 1**, 10-fold excesses of the inorganic species such as Na^+, K^+, Cl^-, NO_3^-, NO_2^-, SO_4^{2-}, ClO_3^-, NH_4^+ and CO_3^{2-} do not interfere with the signal of bromate; while those of Mg^{2+} and Ca^{2+} exhibit interference with the similar degree. The currents of the NENU-3 film electrode for the bromate determination decrease 3% and 4% after the addition of Mg^{2+} and Ca^{2+}, respectively (Table 1). The

Table 1. Effect of possible interfering substances on the NENU-3 film electrode response

Possible interfering substance	Current ratio [a]
Na^+	1
K^+	1
Cl^-	1
NO_3^-	1
NO_2^-	1
SO_4^{2-}	1
ClO_3^-	1
NH_4^+	1
CO_3^{2-}	1
Mg^{2+}	0.97
Ca^{2+}	0.96

[a]Current ratio = $I_{mix}/I_{bromate}$: I_{mix}: the current of mixture of 1 mM interference substance and 0.1 mM bromate; $I_{bromate}$: the current of 0.1 mM bromate alone.

interference of Mg^{2+} and Ca^{2+} may be due to the precipitations produced by the interfering ions (Mg^{2+} and Ca^{2+}) and HPO_4^- and $H_2PO_4^-$ in the buffer solution. The precipitations generated on the surface of the film electrode could hinder electron transfer between the NENU-3 film electrode and bromate, and hence Mg^{2+} and Ca^{2+} slightly interfere with the determination of bromate. Additionally, after the addition of interfering ions, the amperometric i-t response of the film electrode exhibits a decay to a lower steady state value, which is probably related to these interfering ions interaction with the unsaturated coordinated metal centres in the NENU-3 structure as the active center of the electrocatalyst, and thus gradually decreases the current signal of the NENU-3 film electrode for the reduction of bromate.

Conclusions

The electrocatalytically active copper-based NENU-3 film electrodes are fabricated using a facile electrochemical plating method and applied them for the electroanalytical determination of bromate. The film with a thickness of about 4 μm has the high quality crystallinity and homogeneity verified by a series of analysis techniques. Additionally, the electrochemical investigations of the different effects manifest that bromate electroreduction on the NENU-3 film electrode is typical of an irreversible electrode process controlled by diffusion. Taking advantage of the existence of the relatively high effective surface area, the high affinity for bromate and the coordinately unsaturated active sites in the structure, the conductive NENU-3 film is set up for electrochemical sensing towards bromate. The proposed sensor could accurately detect bromate in the range 0.05 ~ 72.74 mM with a detection limit of 12 μM. The interference analysis results show that most of the common co-existing ions in water are no interferences for the determination of bromate. It validates a great application prospect of the NENU-3 film for constructing a high-performance bromate detector. In this context, the electroactive NENU-3 film prepared successfully by electrochemical approach not only provides an effective platform for the assembly of the electroactive MOF films on the conductive substrates, but also holds great promise for the design of electrochemical sensor.

Acknowledgements

The authors acknowledge financial support from the National Natural Science Foundation of China (No. 21471041, No. 21401069, No. 21403048), Natural Science Foundation of Heilongjiang Province of China (No. ZD201214), and PhD Research Startup Program of Harbin Normal University, China (No. XKB201310).

Notes and references

1 Z. Y. Gu, C. X. Yang, N. Chang, X. P. Yan, *Acc. Chem. Res.,* 2012, **45**, 734-745.
2 J. R. Long, O. M. Yaghi, *Chem. Soc. Rev., 2*009, **38**, 1213-1214.
3 M. Eddaoudi, D. F. Sava, J. F. Eubank, K. Adil, V. Guillerm, *Chem. Soc. Rev., 2*015, **44**, 228-249.
4 C. M. Doherty, D. Buso, A. J. Hill, S. Furukawa, S. Kitagawa, P. Falcaro, *Acc. Chem. Res., 2*014, **47**, 396-405.
5 T. Rodenas, I. Luz, G. Prieto, B. Seoane, H. Miro, A. Corma, F. Kapteijn, F. X. Llabrés i Xamena, J. Gascon, *Nat. Mater., 2*015, **14**, 48-55.
6 R. B. Getman, Y. S. Bae, C. E. Wilmer, R. Q. Snurr, *Chem. Rev., 2*012, **112**, 703-723.
7 A. H. Chughtai, N. Ahmad, H. A. Younus, A. Laypkov, F. Verpoort, *Chem. Soc. Rev., 2*015, **44**, 6804-6849.
8 M. D. Allendorf, C. A. Bauer, R. K. Bhakta, R. J. T. Houk, *Chem. Soc. Rev., 2*009, **38**, 1330-1352.
9 A. Bétard, R. A. Fischer, *Chem. Rev., 2*012, **112**, 1055-1083.
10 D. Bradshaw, A. Garai, J. Huo, *Chem. Soc. Rev., 2*012, **41**, 2344-2381.
11 B. Liu, O. Shekhah, H. K. Arslan, J. Liu, C. Wöll, R. A. Fischer, *Angew. Chem. Int. Ed., 2*012, **51**, 807-810.
12 W. Zhang, G. Lu, S. Li, Y. Liu, H. Xu, C. Cui, W. Yan, Y. Yang, F. Huo, *Chem. Commun., 2*014, **50**, 4296-4298.
13 M. E. Silvestre, M. Franzreb, P. G. Weidler, O. Shekhah, C. Wöll, *Adv. Funct. Mater., 2*013, **23**, 1210-1213.
14 P. Ramaswamy, N. E. Wong, G. K. H. Shimizu, *Chem. Soc. Rev., 2*014, **43**, 5913-5932.
15 G. Xu, K. Otsubo, T. Yamada, S. Sakaida, H. Kitagawa, *J. Am. Chem. Soc., 2*013, **135**, 7438-7441.
16 J. Liu, T. Wächter, A. Irmler, P. G. Weidler, H. Gliemann, F. Pauly, V. Mugnaini, M. Zharnikov, C. Wöll, *ACS Appl. Mat. Interfaces* 2015, **7**, 9824-9830.
17 X. Liang, F. Zhang, W. Feng, X. Zou, C. Zhao, H. Na, C. Liu, F. Sun, G. Zhu, *Chem. Sci., 2*013, **4**, 983-992.
18 D. Banerjee, Z. Hu, and J. Li, *Dalton Trans.*, 2014, **43**, 10668-10685.
19 F. Zhang, X. Zou, W. Feng, X. Zhao, X. Jing, F. Sun, H. Ren, G. Zhu, *J. Mater. Chem., 2*012, **22**, 25019-25026.
20 L. E. Kreno, K. Leong, O. K. Farha, M. Allendorf, R. P. Van Duyne, J. T. Hupp, *Chem. Rev., 2*012, **112**, 1105-1125.
21 A. Morozan, F. Jaouen, *Energy Environ. Sci., 2*012, **5**, 9269-9290.
22 Kung, C. W. Chang, T. H. Chou, L. Y. Hupp, J. T. Farha, O. K. Ho, K. C. *Chem. Commun., 2*015, **51**, 2414-2417.
23 S. R. Ahrenholtz, C. C. Epley, A. J. Morris, *J. Am. Chem. Soc., 2*014, **136**, 2464-2472.
24 I. Hod, W. Bury, D. M. Karlin, P. Deria, C. W. Kung, M. J. Katz, M. So, B. Klahr, D. Jin, Y. W. Chung, T. W. Odom, O. K. Farha, J. T. Hupp, *Adv. Mater., 2*014, **26**, 6295-6300.
25 C. W. Kung, T. H. Chang, L. Y. Chou, J. T. Hupp, O. K. Farha, K. C. Ho, *Electrochem. Commun., 2*015, **58**, 51-56.
26 H. Hosseini, H. Ahmar, A. Dehghani, A. Bagheri, A. Tadjarodi, A. R. Fakhari, *Biosens. Bioelectron., 2*013, **42**, 426-429.
27 Y. Zhang, X. Bo, A. Nsabimana, C. Han, M. Li, L. Guo, *J. Mater. Chem. A,* 2015, **3**, 732-738.
28 E. Zhou, Y. Zhang, Y. Li, X. He, *Electroanalysis,* 2014, **26**, 2526-2533.
29 C. Zhang, M. Wang, L. Liu, X. Yang, X. Xu, *Electrochem. Commun.,* 2013, **33**, 131-134.
30 D. M. Fernandes, C. M. Granadeiro, P. M. Paes de Sousa, R. Grazina, J. J. G. Moura, P. Silva, F. A. Almeida Paz, L. Cunha-Silva, S. S. Balula, C. Freire, *ChemElectroChem,* 2014, **1**, 1293-1300.
31 N. Stock, S. Biswas, *Chem. Rev., 2*012, **112**, 933-969.
32 H. Guo, G. Zhu, I. J. Hewitt, S. Qiu, *J. Am. Chem. Soc., 2*009, **131**, 1646-1647.
33 J. Yao, D. Dong, D. Li, L. He, G. Xu, H. Wang, *Chem. Commun., 2*011, **47**, 2559-2561.
34 R. Ameloot, L. Stappers, J. Fransaer, L. Alaerts, B. F. Sels, D. E. De Vos, *Chem. Mater., 2*009, **21**, 2580-2582.
35 M. Li, M. Dinca, *Chem. Sci., 2*014, **5**, 107-111.

36 M. Li, M. Dincă, *J. Am. Chem. Soc., 2*011, **133**, 12926-12929.
37 W. J. Li, J. Lu, S. Y. Gao, Q. H. Li, R. Cao, *J. Mater. Chem. A,* 2014, **2**, 19473-19478.
38 I. Stassen, M. Styles, T. Van Assche, N. Campagnol, J. Fransaer, J. Denayer, J. C. Tan, P. Falcaro, D. De Vos, R. Ameloot, *Chem. Mater.*, 2015, **27**, 1801-1807.
39 B. Van de Voorde, R. Ameloot, I. Stassen, M. Everaert, D. De Vos, J. C. Tan, *J. Mater. Chem. C*, 2013, **1**, 7716-7724
40 A. Martinez Joaristi, J. Juan-Alcañiz, P. Serra-Crespo, F. Kapteijn, J. Gascon, *Cryst. Growth Des.*, 2012, **12**, 3489-3498.
41 I. Hod, W. Bury, D.M. Karlin, P. Deria, C.W. Kung, M.J. Katz, M. So, B. Klahr, D. Jin, Y.W. Chung, *Adv. Mater.*, 2014, **26**, 6295-6300.
42 R. Michalski, A. Łyko, *Crit. Rev. Anal. Chem., 2*013, **43**, 100-122.
43 V. Ingrand, J. L. Guinamant, A. Bruchet, C. Brosse, T. H. M. Noij, A. Brandt, F. Sacher, C. McLeod, A. R. Elwaer, J. P. Croué, P. Quevauviller, *TrAC, Trends Anal. Chem., 2*002, **21**, 1-12.
44 A. Salimi, V. Alizadeh, H. Hadadzadeh, *Electroanalysis,* 2004, **16**, 1984-1991.
45 Q. Li, Q. Zhang, L. Ding, D. Zhou, H. Cui, Z. Wei, J. Zhai, *Chem. Eng. J., 2*013, **217**, 28-33.
46 C. Y. Sun, S. X. Liu, D. D. Liang, K. Z. Shao, Y. H. Ren, Z. M. Su, *J. Am. Chem. Soc., 2*009, **131**, 1883-1888.
47 S. R. Bajpe, C. E. A. Kirschhock, A. Aerts, E. Breynaert, G. Absillis, T. N. Parac-Vogt, L. Giebeler, J. A. Martens, *Chem. Eur. J., 2*010, **16**, 3926-3932.
48 C. H. Hendon, A. Walsh, *Chem. Sci., 2*015, **6**, 3674-3683.
49 N. C. Burtch, H. Jasuja, K. S. Walton, *Chem. Rev., 2*014, **114**, 10575-10612.
50 D. Mustafa, E. Breynaert, S. R. Bajpe, J. A. Martens, C. E. A. Kirschhock, *Chem. Commun., 2*011, **47**, 8037-8039.
51 Y. Zhang, A. Nsabimana, L. Zhu, X. Bo, C. Han, M. Li, L. Guo, *Talanta* 2014, **129**, 55-62.
52 Y. Liu, X. Yang, J. Miao, Q. Tang, S. Liu, Z. Shi, S. Liu, *Chem. Commun.*, 2014, **50**, 10023-10026.
53 A. J. Bard, L. R. Faulkner, *Electrochemical methods: fundamentals and applications*. Wiley New York: 1980 Vol., 2.
54 E. Laviron, *J. Electroanal. Chem. Interfacial Electrochem.* 1979, **101**, 19-28.
55 D. D. Zhou, L. Ding, H. Cui, H. An, J. P. Zhai, Q. Li, *Chem. Eng. J., 2*012, **200-202**, 32-38.
56 F. C. Anson, *Anal. Chem.* 1964, **36**, 932-934.
57 M. Zhou, L. P. Guo, F. Y. Lin, H. X. Liu, *Anal. Chim. Acta* 2007, **587**, 124-131.
58 M. Majidi, S. Ghaderi, K. Asadpour-Zeynali, H. Dastangoo, *Food Anal. Methods,* 2015, **8**, 2011-2019.
59 C. Chen, Y. Song, L. Wang, *Electrochim. Acta,* 2009, **54**, 1607-1611.
60 Y. Li, S. M. Chen, R. Thangamuthu, M. Ajmal Ali, F. M. A. Al-Hemaid, *Electroanalysis,* 2014, **26**, 996-1003.
61 Y. Zhang, F. Wen, Y. Jiang, L. Wang, C. Zhou, H. Wang, *Electrochim. Acta,* 2014, **115**, 504-510.